

# Supporting information for “Graphenylene, a unique two-dimensional carbon network with nondelocalized cyclohexatriene units”

Qi Song<sup>1</sup>, Bing Wang<sup>1</sup>, Ke Deng<sup>1</sup>, Xinliang Feng<sup>2</sup>, Manfred Wagner<sup>2</sup>, Julian D. Gale<sup>3\*</sup>, Klaus Müllen<sup>2</sup>,  
and Linjie Zhi<sup>1\*</sup>

<sup>1</sup> National Center for Nanoscience and Technology, No.11 Beiyitiao Zhongguancun, 100190 Beijing, P.R. China

<sup>2</sup> Max Plank Institute for Polymer Research, Mainz, Germany

<sup>3</sup> Department of Chemistry/Nanochemistry Research Institute, Curtin University, PO Box U1987, Perth, WA 6845, Australia

\*To whom correspondence should be addressed

E-mail: [J.Gale@curtin.edu.au](mailto:J.Gale@curtin.edu.au), [zhilj@nanoctr.cn](mailto:zhilj@nanoctr.cn)

## 1. Computational methods

The first-principles calculations, based on Kohn-Sham density functional theory (DFT), were performed within the plane-wave pseudopotential method<sup>i</sup> using the CASTEP program.<sup>ii</sup> Ultrasoft pseudopotentials<sup>iii</sup> were used to represent the combined effective potential of the core electrons and nuclei, and a plane-wave cut-off of 310 eV was used for systems containing only carbon, while for those containing oxygen this was increased to 380 eV. Three different functionals were used to explore the sensitivity of the results with respect to this choice; namely, the local density approximation (LDA), the Perdew-Burke-Ernzerhof (PBE) generalized gradient approximation (GGA)<sup>iv</sup> and the PBEsol variant of this functional.<sup>v</sup> Geometry optimization was performed until all the atomic forces are less than 0.01 eV/Å. The phonon dispersion curves were computed using the linear-response approach with the PBEsol functional. The electron density, band structure and energy calculation was also completed by PBEsol functional while the calculation of gas separation was computed using the PBE functional. The supercell used was large enough to ensure that the width of vacuum gap between two sheets is more than 15 Å, thereby leading to minimal artificial interaction between images. Similarly the sampling of the Brillouin zone with a Monkhorst-Pack mesh<sup>vi</sup> was increased to ensure sufficient precision of the results.

**Table S1.** Lattice parameters, bonds length and band gap of graphenylene with different functionals (Bond-1 is the double bond in the hexatomic ring, bond-2 is the single bond in the hexatomic ring and bond-3 is the single bond outside the hexatomic ring)

	Lattice parameters (Å)	Bond-1 (Å)	Bond-2 (Å)	Bond-3 (Å)	Band gap (eV)
<b>LDA</b>	$a=b=6.70$	1.353	1.456	1.463	0.010
<b>PBE</b>	$a=b=6.76$	1.365	1.469	1.479	0.054
<b>PBEsol</b>	$a=b=6.76$	1.366	1.467	1.478	0.025

## 2. Comparison of geometry optimization results with different functionals

The results of the geometry optimization of graphenylene are given in Table S1. As would be expected from its tendency to overbind, the LDA functional yields the smallest lattice parameters, leading to a commensurate overall shortening of the bond lengths. Similarly, the PBE results are likely to represent an overestimate of the bond lengths. All three functionals exhibit the same large variation of the bond lengths within the hexatomic rings, consistent with non-delocalized bonding. The results for the calculation of the Kohn-Sham band gap are also shown in Table S1. We note that since the Kohn-Sham eigenvalues contain a self-interaction error, the magnitude of the band gap is almost certainly a lower bound to the true value.

### 3. Phonon dispersion curves along selected directions within the Brillouin zone of graphenylene.

The phonon dispersion curves for graphenylene demonstrate the absence of any imaginary frequencies, and therefore the structure is a genuine local minimum on the potential energy surface, and capable of existing in reality.

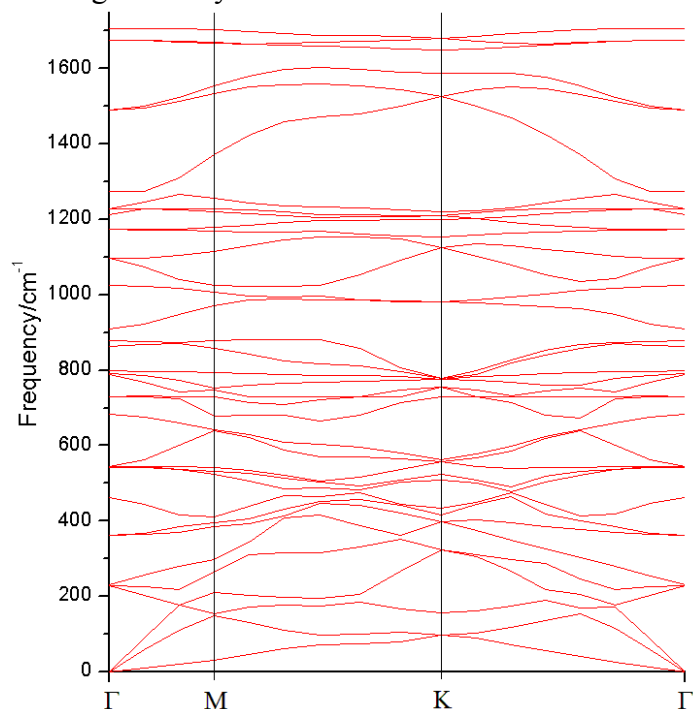


Figure S1. Phonon dispersion curves along selected directions within the Brillouin zone of graphenylene.

### 4. Theoretical explanation of the existence of cyclohexatriene units in graphenylene.

According to resonance theory, we can give an intuitive explanation for the formation of cyclohexatriene. Benzene has two stable canonical forms that contribute equally to the resonance hybrid. So the six C-C bonds in benzene have the same length and the same electron density. In graphenylene, with tetratomic rings, the energies of canonical forms (a), (c), (d) and (e) are much higher than that of canonical form (b) because of the existence of either cyclobutene or cyclobutadiene units (Fig.S2). As the lowest energy configuration, canonical form (b) is therefore the dominant contributor to the resonance hybrid. For this reason, cyclohexatriene represents the appropriate description of the electronic structure present in the six-rings of graphenylene, rather than benzene.

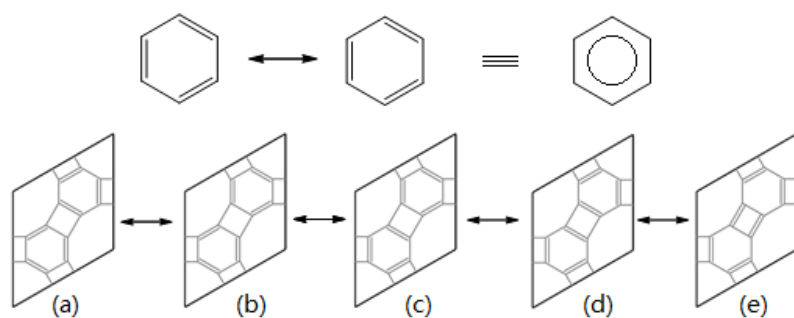
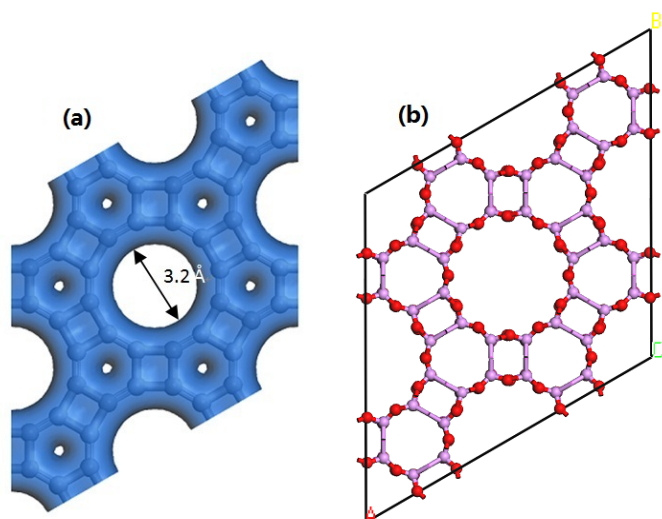


Figure S2. Resonance between canonical forms of benzene and graphenylene

### 5. Structures of graphenylene and AFL.

According to simulation results of Figure S3, graphenylene has a two-dimensional mesh with periodically distributed pores of 3.2 Å in diameter.



**Figure S3.** (a) The electron density isosurface for graphenylene where the isovalue is 0.2 a.u. and (b) the view along the [001] direction of AFI with T sites and oxygen in pink and red, respectively. Both graphenylene and AFI are 4,6,12 conjoined networks.

## 6. Estimation of the selectivity of gas separation by graphenylene with the Arrhenius equation.

The selective for diffusion of hydrogen through graphenylene relative to some other gas, G, can be estimated using transition state theory (neglecting any tunneling contribution) with the following equation:

$$S_{\text{H}_2/\text{G}} = \frac{D_{\text{H}_2}}{D_{\text{G}}} = \frac{A_{\text{H}_2}}{A_{\text{G}}} \frac{e^{-E_{\text{H}_2}/RT}}{e^{-E_{\text{G}}/RT}}$$

S-Selectivity

D-Diffusion rate

A-Diffusion prefactor

E-Diffusion barrier

For simplicity, we consider  $T=300$  K and assume the diffusion prefactor for both gases will be the same. In reality the prefactor is likely to vary as the inverse square root of the mass of the molecule, based on a simple collision theory. However, since this gives a maximum prefactor ratio of  $\sim 4.7$  for  $\text{H}_2$  to  $\text{CO}_2$ , and we only report selectivities to the nearest order of magnitude, any variation is relatively insignificant.

The diffusion barrier ( $E_{\text{G}}-E_{\text{H}_2}$ ) of different gases and the separation selectivity of hydrogen relative to the other gases is listed in Table S2. The diffusion barrier of each molecule was calculated according to the equation:

$$E = E_{\text{pore}} - E_{\text{graphenylene}} - E_{\text{gas}}$$

Here  $E_{\text{pore}}$  is the energy of the gas molecule placed in a symmetric position within the pore of graphenylene and fully relaxed, while  $E_{\text{graphenylene}}$  and  $E_{\text{gas}}$  are the energies of the isolated graphenylene and gas molecule, respectively. We note that this approach represents an approximation to the true activation energy of diffusion since it neglects the role of any physisorbed minima prior to diffusion, as well as the vibrational, translational and rotational contributions to the free energy of activation. However, since many of these corrections will be similar for the different molecules and smaller in magnitude than

the internal energy differences, the selectivities predicted should represent a reliable indication of the ability of graphenylene to separate hydrogen from the other gases considered.

**Table S2.** Relative diffusion barrier compared with H<sub>2</sub> and the separation selectivity of H<sub>2</sub>/G

	CO	N <sub>2</sub>	CO <sub>2</sub>	CH <sub>4</sub>
<b>Relative diffusion barrier (eV)</b>	0.79	0.81	0.85	2.08
<b>Separation selectivity</b>	10 <sup>12</sup>	10 <sup>13</sup>	10 <sup>13</sup>	10 <sup>34</sup>

### 7. The simulated electron diffraction image of single layer graphenylene.

A simulated transmission electron diffraction image of single layer graphenylene is shown in Fig. S4. This may help us to find evidence for the existence of graphenylene experimentally.

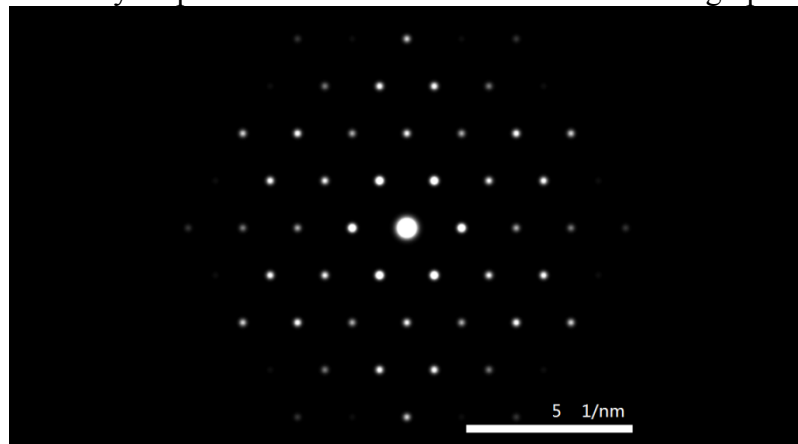


**Figure S4.** The simulated electron diffraction image of single layer

<sup>i</sup> Payne, M.C.; Teter, M.P.; Allan, D.C.; Arias, T.A.; Joannopoulos, J.D. *Rev. Mod. Phys.*, **1992**, *64*, 1045-1097.

<sup>ii</sup> Clark, S.J.; Segall, M.D.; Pickard, C.J.; Hasnip, P.J.; Probert, M.J.; Refson, K.; Payne, M.C. *Z. Krist.*, **2005**, *220*, 567-570.

<sup>iii</sup> Vanderbilt, D. *Phys. Rev. B*, **1990**, *41*, 7892-7895.

<sup>iv</sup> Perdew, J. P.; Burke, K.; Ernzerhof, M. *Phys. Rev. Lett.* **1996**, *77* (18), 3865-3868.

<sup>v</sup> Perdew, J. P.; Ruzsinszky, A.; Csonka, G. I.; Vydrov, O. A.; Scuseria, G. E.; Constantin, L. A.; Zhou, X.; Burke, K. *Phys. Rev. Lett.* **2008**, *100*(13), 136406.

<sup>vi</sup> Monkhorst, H.J.; Pack, J.D. *Phys. Rev.* **1976**, *13*, 5188.